



Contents lists available at ScienceDirect

Deep-Sea Research II

journal homepage: www.elsevier.com/locate/dsr2

Impact of glider data assimilation on the Monterey Bay model

Igor Shulman^{a,*}, Clark Rowley^a, Stephanie Anderson^a, Sergio DeRada^a, John Kindle^a, Paul Martin^a, James Doyle^b, James Cummings^a, Steve Ramp^c, Francisco Chavez^d, David Fratantoni^e, Russ Davis^f^a Oceanography Division, Naval Research Laboratory, Stennis Space Center, MS 39529, USA^b Marine Meteorology Division, Naval Research Laboratory, Monterey, CA 93943, USA^c Department of Oceanography, Naval Postgraduate School, Monterey, CA 93943, USA^d MBARI, 7700 Sandholdt Road, Moss Landing, CA 95039, USA^e Woods Hole Oceanographic Institution, Woods Hole, MA, USA^f Scripps Institution of Oceanography, La Jolla, CA, USA

ARTICLE INFO

Article history:

Accepted 17 August 2008

Keywords:

Ocean data assimilation and reanalysis
Coastal processes
Ocean predictability and prediction
Ocean observing systems
Upwelling

ABSTRACT

Glider observations were essential components of the observational program in the Autonomous Ocean Sampling Network (AOSN II) experiment in the Monterey Bay area during summer of 2003. This paper is focused on the impact of the assimilation of glider temperature and salinity observations on the Navy Coastal Ocean Model (NCOM) predictions of surface and subsurface properties. The modeling system consists of an implementation of the NCOM model using a curvilinear, orthogonal grid with 1–4 km resolution, with finest resolution around the bay. The model receives open boundary conditions from a regional (9 km resolution) NCOM implementation for the California Current System, and surface fluxes from the Coupled Ocean–Atmosphere Mesoscale Prediction System (COAMPS) atmospheric model at 3 km resolution. The data assimilation component of the system is a version of the Navy Coupled Ocean Data Assimilation (NCODA) system, which is used for assimilation of the glider data into the NCOM model of the Monterey Bay area. The NCODA is a fully 3D multivariate optimum interpolation system that produces simultaneous analyses of temperature, salinity, geopotential, and vector velocity.

Assimilation of glider data improves the surface temperature at the mooring locations for the NCOM model hindcast and nowcasts, and for the short-range (1–1.5 days) forecasts. It is shown that it is critical to have accurate atmospheric forcing for more extended forecasts. Assimilation of glider data provided better agreement with independent observations (for example, with aircraft measured SSTs) of the model-predicted and observed spatial distributions of surface temperature and salinity. Mooring observations of subsurface temperature and salinity show sharp changes in the thermocline and halocline depths during transitions from upwelling to relaxation and vice versa. The non-assimilative run also shows these transitions in subsurface temperature; but they are not as well defined. For salinity, the non-assimilative run significantly differs from the observations. However, the glider data assimilating run is able to show comparable results with observations of thermocline as well as halocline depths during upwelling and relaxation events in the Monterey Bay area. It is also shown that during the relaxation of wind, the data assimilative run has higher value of subsurface velocity complex correlation with observations than the non-assimilative run.

© 2008 Elsevier Ltd. All rights reserved.

1. Introduction

Five Spray gliders (Sherman et al., 2001) and 10 Slocum gliders (Webb et al., 2001) were deployed in the Autonomous Ocean Sampling Network (AOSN II) experiment in the Monterey Bay area during August–September 2003 (www.mbari.org/aosn/Monterey-Bay2003). Spray gliders collected temperature and salinity

profiles up to 400 m depth (with occasional profiles to 700 m for instrument comparison with other measurements) from Point Año Nuevo in the north to Point Sur in the south, while the Slocum gliders profiled to 200 m closer to shore (Fig. 1). A detailed description of glider operations and data collected during the AOSN II experiment can be found in Ramp et al. (2008).

The focus of the present paper is on the impact of the assimilation of glider temperature and salinity observations on the Navy Coastal Ocean Model (NCOM) predictions of surface and subsurface properties. Model predictions are evaluated and compared with the observed data (temperature, salinity, currents)

* Corresponding author.

E-mail address: igor.shulman@nrlssc.navy.mil (I. Shulman).

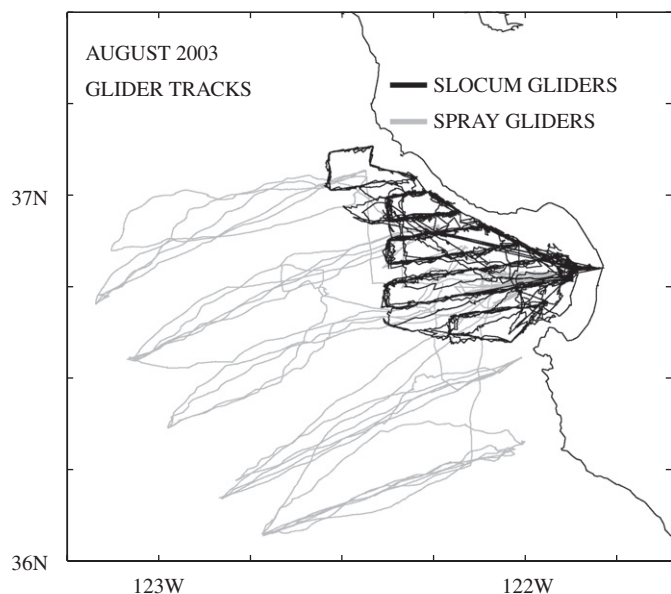


Fig. 1. Glider tracks during August 2003.

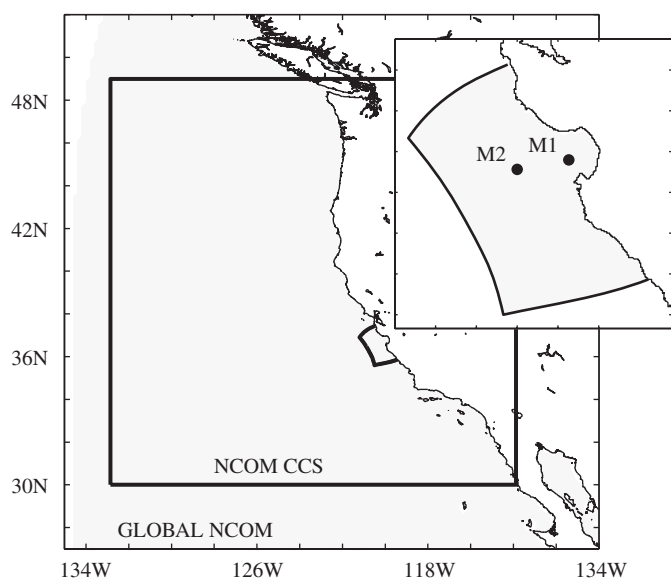


Fig. 2. Hierarchy of nested NCOM models along US west coast.

at two mooring locations M1 and M2 (Fig. 2), and with airborne SSTs. Temperature and salinity at the moorings were measured by a string of 12 SeaBird MicroCAT TCP recorders. Observed currents were measured by a 75-kHz RD Instruments acoustic Doppler current profiler (ADCP) mounted in a downward-looking configuration on the moorings. For the considered time frame, the ADCPs were set up to measure in 8-m depth bins with 60 depth bins, with the first bin at 16 m for both moorings. A detailed description of the airborne SST observations can be found in Ramp et al. (2008).

The impact of glider data assimilation is evaluated during observed upwelling and relaxation events. During northwesterly, upwelling-favorable winds, the hydrographic conditions in and around the Monterey Bay are mostly determined by the interaction between upwelling filaments formed at headlands to the north (Point Año Nuevo) and south of the bay (Point Sur) and the anticyclonic California Current meander offshore of the bay. When

upwelling-favorable winds weaken (wind relaxation) and sometimes become poleward, the anticyclonic meander moves onshore and then quickly retreats back offshore when the winds re-intensify. The flow at the surface is mostly southward due to local upwelling wind and the influence of the offshore California Current. Two narrow, poleward-flowing boundary currents were observed around the Monterey Bay area: the inshore counter-current (sometimes called the Davidson Current) and the California Undercurrent (CU). For more details on observed physical conditions in the area see, for example, Rosenfeld et al. (1994) and Ramp et al. (2005, 2008).

2. Modeling system

In the present study, the Monterey Bay model is based on the NCOM (Rhodes et al., 2002; Martin, 2000), and is triply nested inside of the global and regional (California Current) NCOM-based models (Shulman et al., 2004, 2007). The model is called NCOM ICON due to the fact that initial development of the model started under the National Oceanic Partnership Program (NOPP) Innovative Coastal-Ocean Observing Network (ICON) project (Shulman et al., 2002, 2007; Ramp et al., 2005). The model, which is set up on a curvilinear orthogonal grid with resolution ranging from 1 to 4 km, uses a sigma vertical coordinate system with 30 levels. The model is forced with surface fluxes from the Coupled Ocean-Atmosphere Mesoscale Prediction System (COAMPS) atmospheric

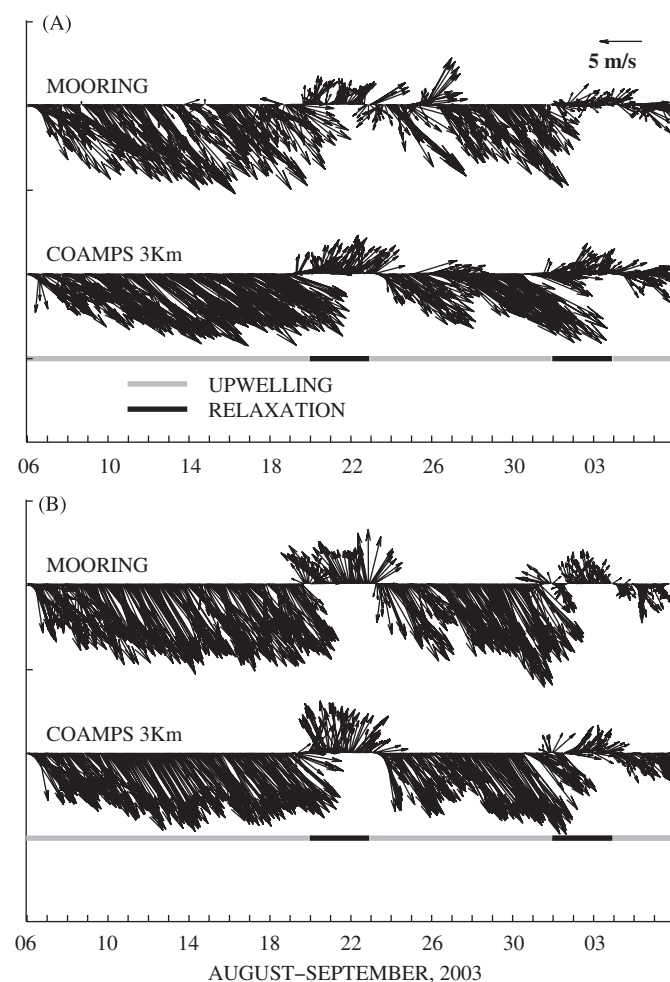


Fig. 3. Observed and COAMPS-predicted wind velocities at M1 (A) and M2 (B) moorings.

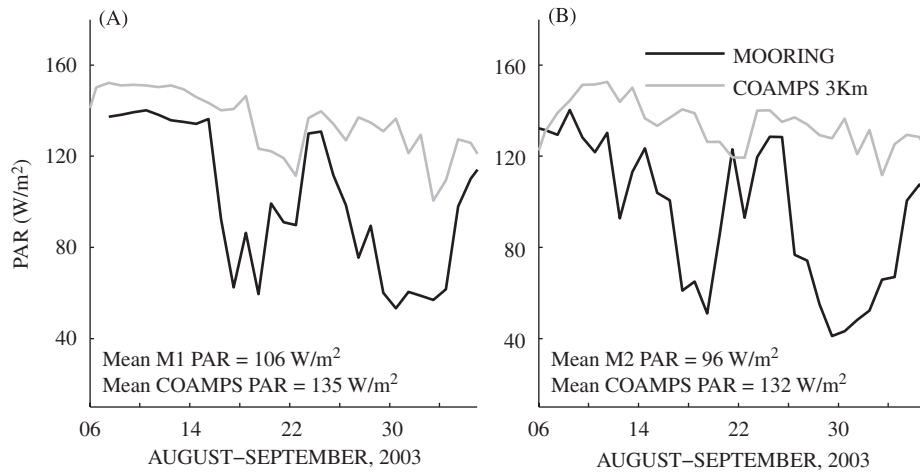


Fig. 4. Observed and COAMPS derived PAR at M1 (A) and M2 (B) moorings.

Table 1

Description of NCOM runs together with comparisons of SST predictions at moorings

Run	SWR correction	Glider assimilation	M1 relaxation event (August 20–23, 2003)		M2 upwelling event (August 6–19, 2003)	
			BIAS (°C)	RMS (°C)	BIAS (°C)	RMS (°C)
1	None	None	1.7	2.15	−0.7	1.03
2	Yes	None	0.4	0.95	−1.2	1.40
3	None	Yes	−0.5	1.12	0.4	0.81
4	Yes	Yes	−0.6	0.97	0.3	0.80

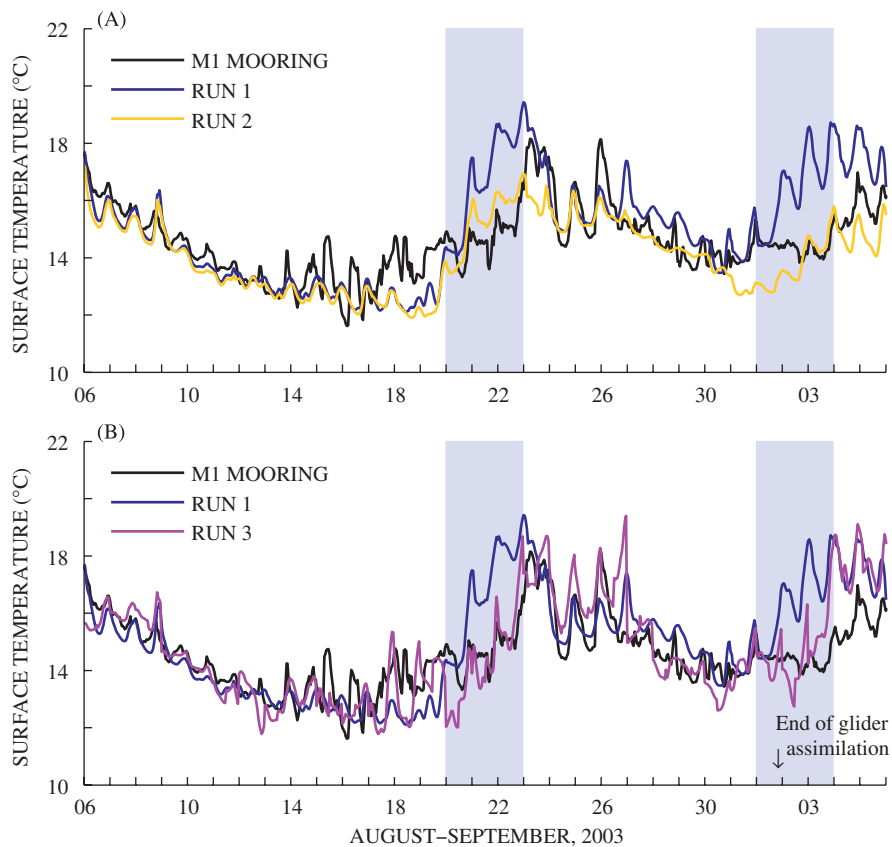


Fig. 5. Observed and model-predicted SSTs at mooring M1. (A) Comparisons between Runs 1 and 2 (Table 1). (B) Comparisons between Runs 1 and 3 (Table 1).

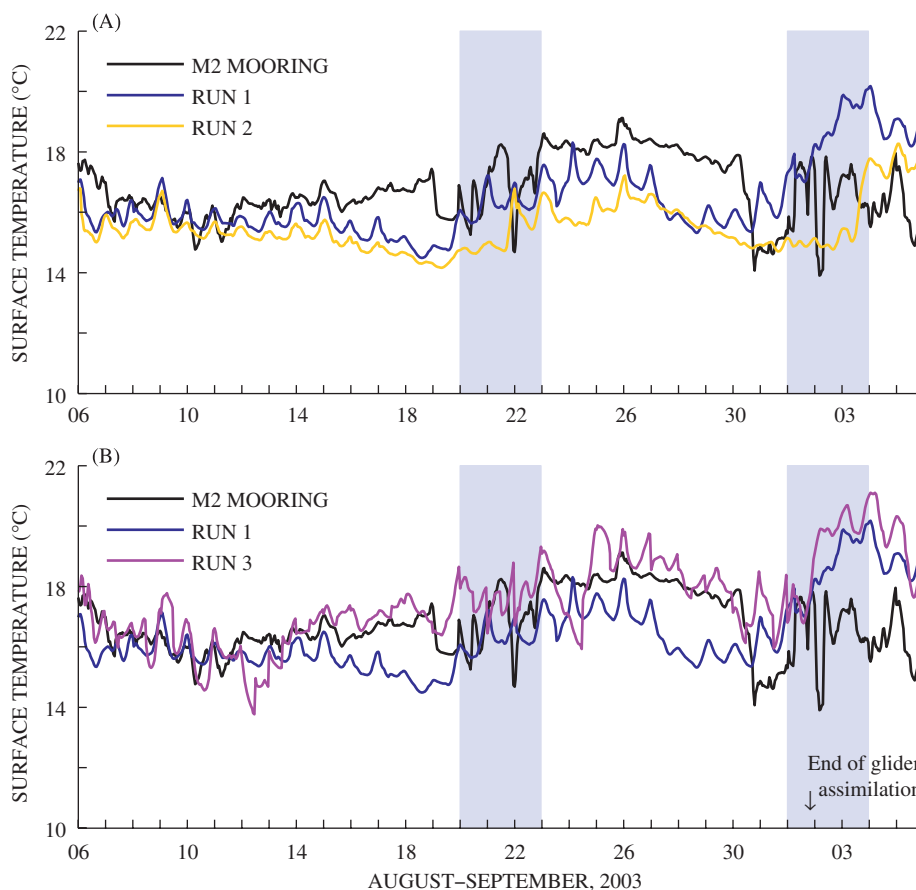


Fig. 6. Same as Fig. 5 but at mooring M2.

model at 3 km horizontal resolution. The NCOM ICON model uses the Mellor–Yamada level 2.5 turbulence closure scheme, and the Smagorinsky formulation is used for horizontal mixing (Martin 2000). On open boundaries, the model is one-way coupled to a larger scale regional (California Current) NCOM-based model (Shulman et al., 2007).

In this study, the Navy Coupled Ocean Data Assimilation (NCODA) system (Cummings, 2006) is used for assimilation of the glider data into the NCOM ICON model. The NCODA is a fully 3D multivariate optimum interpolation system that produces simultaneous analyses of temperature, salinity, geopotential, and vector velocity. The system uses the background error covariances, which represent a product of background error variance and a correlation. Correlations are a product of horizontal and vertical correlations, which are modeled by the second order autoregressive (SOAR) functions (Cummings, 2006). Background error variances vary with position, depth, and analysis variables, and evolve over time based on a time history of the differences between NCODA analysis and the model forecast fields (Cummings, 2006). Observation errors and background errors are assumed to be uncorrelated, and errors associated with observations made at different locations and at different times are also assumed to be uncorrelated. Assimilation of temperature and salinity data is performed every 12 h (assimilation cycle). Differences between the NCODA analysis and the model forecast are uniformly added to the model temperature and salinity fields over the assimilation cycle. Temperature and salinity data from each descent/ascent glider path from a particular dive are treated as vertical profiles of temperature and salinity. This introduces additional error into the glider data assimilation, because glider paths have angles sometimes reaching 26° . Spray gliders collected

data with a nominal spatial resolution of 2.3 km, and Slocum gliders with resolution of 0.8 km. According to the model resolution, the spatial error in treating gliders as vertical profiles does not exceed one model grid point. At the same time, assimilation of glider data as threaded profiles (when each glider profile has latitude and longitude values changing with the depth) is a topic of our future research.

3. Atmospheric forcing

Atmospheric fields from the 3-km resolution COAMPS predictions are used in this study (Doyle et al., 2008). COAMPS assimilates atmospheric observations from radiosondes, aircraft, satellite, and ships. The COAMPS SST analysis is performed directly on the particular nest grid and includes assimilation of observations from ships, buoys, satellites (for example, multi-channel sea surface temperature (MCSST)). Atmospheric, as well as oceanic observations from moorings M1 and M2 (Fig. 2) were not assimilated into the COAMPS simulations.

Comparisons of observed and COAMPS-predicted wind velocities at the M1 and M2 moorings are presented in Fig. 3. Complex correlations and angular displacements (estimated according to Kundu, 1976) between the observed wind velocity and the COAMPS-predicted wind velocities were also estimated. The angular displacement gives the average counterclockwise angle of the COAMPS wind velocity with respect to the observed wind velocity. COAMPS predictions show a high correlation with observations (larger than 0.79) and small angles of displacements. There is good agreement between COAMPS-predicted winds and observations in the sequence and extent of

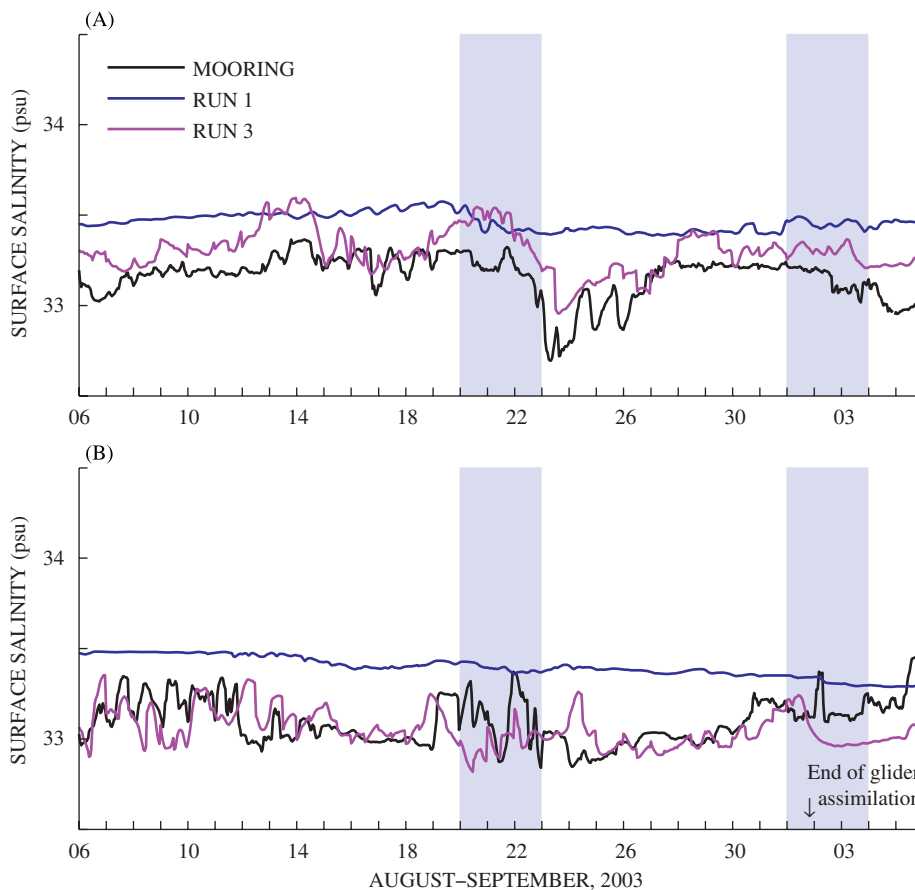


Fig. 7. Observed and model-predicted surface salinities at moorings M1 (A) and M2 (B).

each upwelling–relaxation event that occurs between August 6 and September 6 of 2003. These events include an extended upwelling period from August 6 to 19, a brief relaxation from August 20 to 22, followed by a second extended upwelling event between August 23 and 31, and ending with a short relaxation (September 1–3) and weak upwelling (September 4–6) periods (see also Ramp et al., 2008).

Daily-averaged, photosynthetically available radiation (PAR) observed at M1 and M2 and estimated from the COAMPS short wave radiation (SWR) fluxes are presented in Fig. 4. The observed PAR was measured by the Biospherical PRR-620 spectroradiometer mounted on moorings approximately 3 m above the water surface (Chavez et al., 2000). PAR from COAMPS predictions was estimated as 45% of the COAMPS-predicted SWR flux (Strutton and Chavez, 2004). From the observed and model-predicted mean values presented in Fig. 4, it is clear that there is an overestimation of the SWR in the COAMPS predictions. A similar overestimation of SWR by COAMPS predictions was documented during August of 2000 (Shulman et al., 2007). The excessive SWR is likely related to the modeling of low-level clouds. Predictions of extensive low-level clouds in the Monterey Bay area during summer, which are believed to be underestimated by COAMPS during this time period (Doyle et al., 2008) is a very challenging problem.

4. Results

Table 1 lists the attributes of the NCOM ICON runs that are evaluated in the paper. All model runs were initialized on August 2, 2003 from the same NCOM CCS model fields and spun up

with COAMPS surface fluxes, tides, and NCOM CCS fields on the open boundaries. The NCOM ICON predictions during August 6–September 6 are evaluated.

4.1. Impact of glider data assimilation on the model prediction of surface properties

Comparisons of the observed and model-predicted SSTs from the base, non-data assimilative Run 1 (Table 1) are shown in Fig. 5A for mooring M1. Model predictions are capable of reproducing the observed sequence of upwelling/relaxation events and are in reasonably good agreement with observations during upwelling events. This can be attributed, in part, to the good agreement between observed and COAMPS-predicted winds (Fig. 3). However, there are substantial differences between model and observations during short relaxation events of August 20–22 and September 1–3. The model-predicted SSTs are much warmer than observed SSTs, and there is stronger diurnal variability in the model-predicted SSTs. This is consistent with results reported in Shulman et al. (2007), in which it was demonstrated that the model predictions were consistent with observations during upwelling events of August 2000, and were considerably different during the relaxation events. It was shown that the oceanic model deficiencies in predictions of observed SSTs during wind relaxation events are correlated strongly with the fact that the COAMPS-predicted mean SWR flux was around 40% larger than observed values at mooring locations. There is also a similar overestimation of SWR during August of 2003 (Fig. 4). In Shulman et al. (2007), it was recommended that the COAMPS SWR field be adjusted toward the observed values at moorings. In Run 2 (Table 1), the

mean daily values of COAMPS SWR were replaced by the observed mean daily values of SWR at mooring M1. The correction of SWR improved the Run 2 predictions during the relaxation events (Fig. 5A). According to Table 1, SST bias is reduced from 1.7 (Run 1) to 0.4 °C (Run 2), and root mean square error (RMS) is reduced to half. This is similar to results presented in Shulman et al. (2007) for August of 2000.

The assimilation of glider data in Run 3 with the same uncorrected atmospheric forcing as in Run 1 (Table 1) substantially improved the model predictions in comparison to the base Run 1 during the relaxation event of August 20–22 (Fig. 5B). The data assimilative Run 3 and Run 2 (with corrected atmospheric forcing) have comparable SST biases and RMS errors (Table 1). Glider assimilation ends around September 2 (with a much smaller number of data profiles available for assimilation during September 1–2 than in August of 2003). Fig. 5B shows that for 1–1.5 days after glider data assimilation ends, the SSTs from data assimilative Run 3 are similar to SSTs from non-assimilative Run 1. This shows that while the hindcasts and nowcasts are improved with assimilation of the glider observations, the SSTs forecast degrades to the level of the model predictions without assimilation in 1–1.5 days. It is demonstrated below (Run 4, Table 1) that for more extended forecasts, it is critical to have accurate atmospheric forcing.

The model predictions also were evaluated at the M2 location. Mooring M2 is located farther offshore than mooring M1 and in an area that is significantly affected by onshore and offshore

migration of the anticyclonic Monterey Bay Eddy (MBE) (Rosenfeld et al., 1994; Ramp et al., 2005). There are SST differences between the base Run 1 and the observed SST at the end of the upwelling event (August 6–19) (Fig. 6A). During this time, the model has colder SSTs than observed with the bias around -0.7 °C (Table 1). For this reason, the reduction of SWR in Run 2, which improved the predictions at M1 during the relaxation events, makes the SST even colder at M2 during the upwelling events (Fig. 6A), and SST bias for Run 2 is around -1.2 °C (Table 1). At the same time, the assimilation of glider data in Run 3 improved the model SST predictions at M2 during the upwelling events (Fig. 6B). During the upwelling of August 6–19, the SST bias was reduced to 0.4 °C from -0.7 °C for the base Run 1 (Table 1).

Observed and model-predicted surface salinities are compared in Fig. 7. The assimilation of glider data significantly improved the model salinity predictions in comparison to the non-assimilative run, especially at the mooring M2 location (Fig. 7).

The impact of glider data assimilation on spatial distributions of surface properties of temperature and salinity (SSS) are illustrated in Figs. 8 and 9. Observed airborne SSTs (Ramp et al., 2008) and model-predicted surface temperature and salinity are shown for two upwelling events of August 15 (Fig. 8) and August 29 (Fig. 9). During both upwelling events, the non-assimilative Run 1 has water masses warmer than 17° farther offshore than in the observations. Assimilation of glider data provided a better agreement of the model-predicted and observed spatial distributions of SSTs properties, as for example, in location of warmer

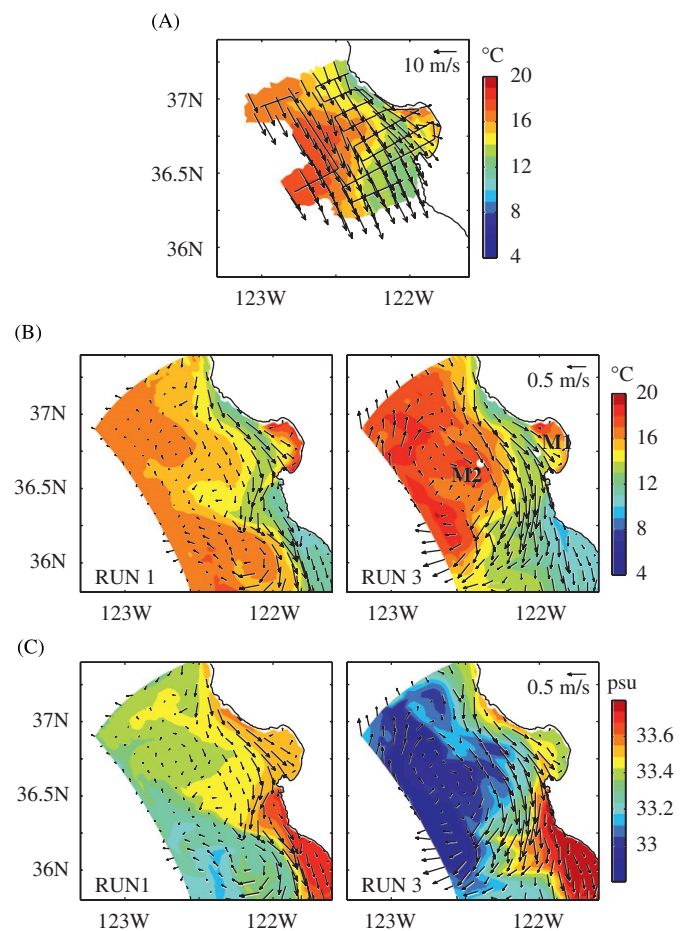


Fig. 8. Comparisons of aircraft and model-predicted SSTs for August 15, 2003. (A) Aircraft measured SSTs with wind velocities overlay. (B) Model-predicted SSTs and surface currents for Runs 1 and 3. (C) Model-predicted surface salinity and currents for Runs 1 and 3.

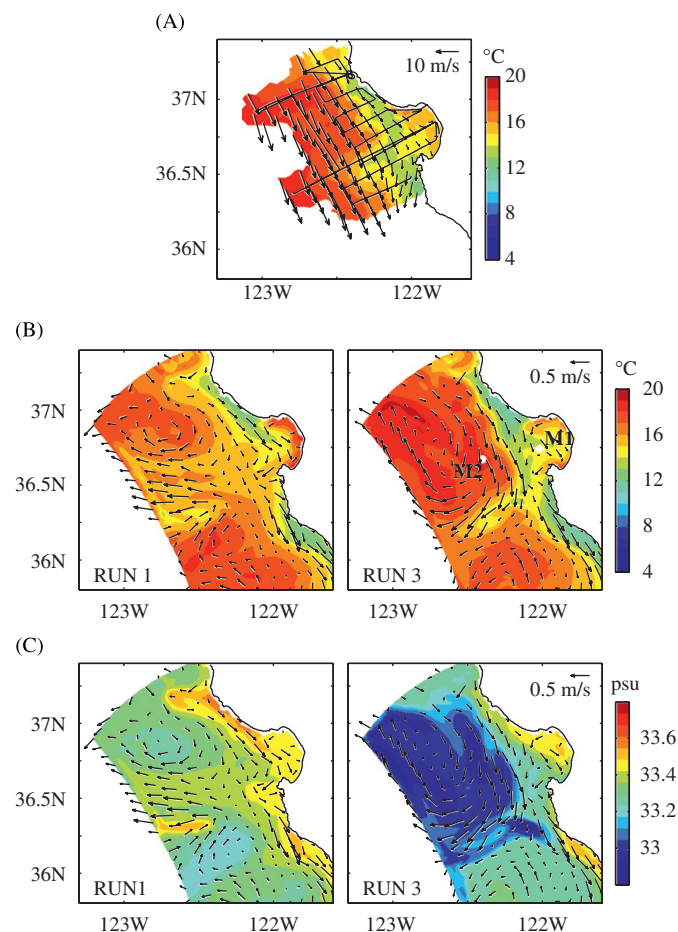


Fig. 9. Same as Fig. 8 but for August 29, 2003.

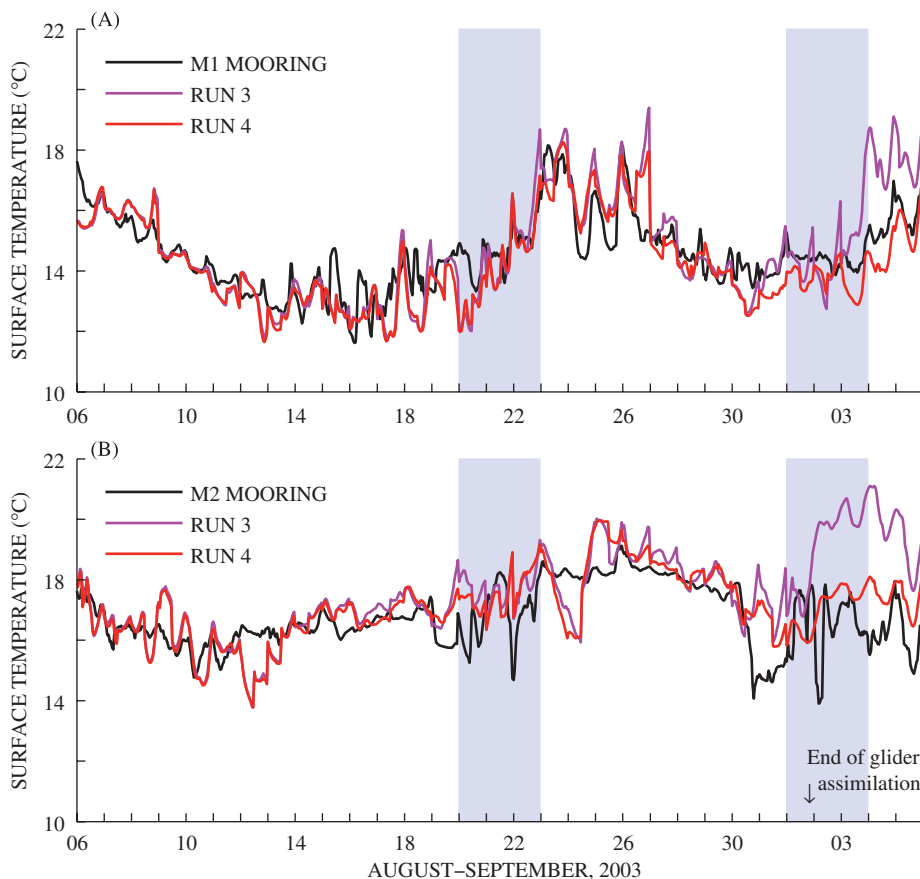


Fig. 10. Comparisons of observed and model-predicted SSTs at moorings M1 (A) and M2 (B).

Table 2

Comparison of SSTs at M1 and M2 during September 3–6, 2003

Run	M1		M2	
	BIAS (°C)	RMS (°C)	BIAS (°C)	RMS (°C)
1	1.6	2.08	2.5	2.75
2	−0.9	1.27	0.9	1.69
3	1.4	1.72	3.5	3.63
4	−1.0	1.08	1.4	1.54

offshore water masses (Figs. 8 and 9). This resulted in fresher water masses closer to shore in Run 3 than in Run 1, which improved surface salinity predictions at M1 and M2 moorings (Fig. 7).

Model Run 4 (Table 1) is similar to Run 3 but with correction of the SWR field as in Run 2. The SSTs at M1 and M2 for Runs 3 and 4 are very similar during the period of glider data assimilation. The correction of SWR improved the model predictions at the end of the evaluation period (September 3–6, transition from relaxation to upwelling and when the glider data were not available for assimilation) (Fig. 10, Table 2). In comparison to Run 3, the correction of SWR improves the model SSTs forecasts beyond 1.5 days for Run 4. This supports the above statement that assimilation of glider data improves model SSTs hindcasts and nowcasts, and short-range (1–1.5 day) forecasts. However, for more extended forecasts it is critical to have accurate atmospheric forcing. Correction of SWR in accord with mooring observations improves model SSTs predictions.

Table 3

Comparison of surface temperature and salinity for the entire period of assimilation

Run	Temperature				Run	Salinity			
	M1		M2			M1		M2	
	BIAS	RMS	BIAS	RMS		BIAS	RMS	BIAS	RMS
1	0.24	1.18	−0.69	1.30	1	0.30	0.32	0.32	0.34
3	−0.11	0.91	0.68	1.36	3	0.15	0.18	−0.04	0.14

Table 3 presents a comparison between Runs 1 and 3 over the entire period of assimilation. The biases and RMS errors in surface salinity are reduced by more than 50% for the data assimilative run at both moorings (Table 3). At mooring M1, statistics for temperature are also improved with assimilation, while at mooring M2, temperature statistics for both runs are comparable.

4.2. Impact of glider data assimilation on the model predictions of subsurface properties

The impact of glider data assimilation on model subsurface temperature and salinity at M1 and M2 are shown in Figs. 11 and 12. There are distinct changes in the thermocline and halocline depths during transitions from upwelling to relaxation and vice versa (top panels on Figs. 11 and 12). At M2, there is a strong deepening of the thermocline during the upwelling events of August 6–19 and 23–31, and a shallowing of the thermocline

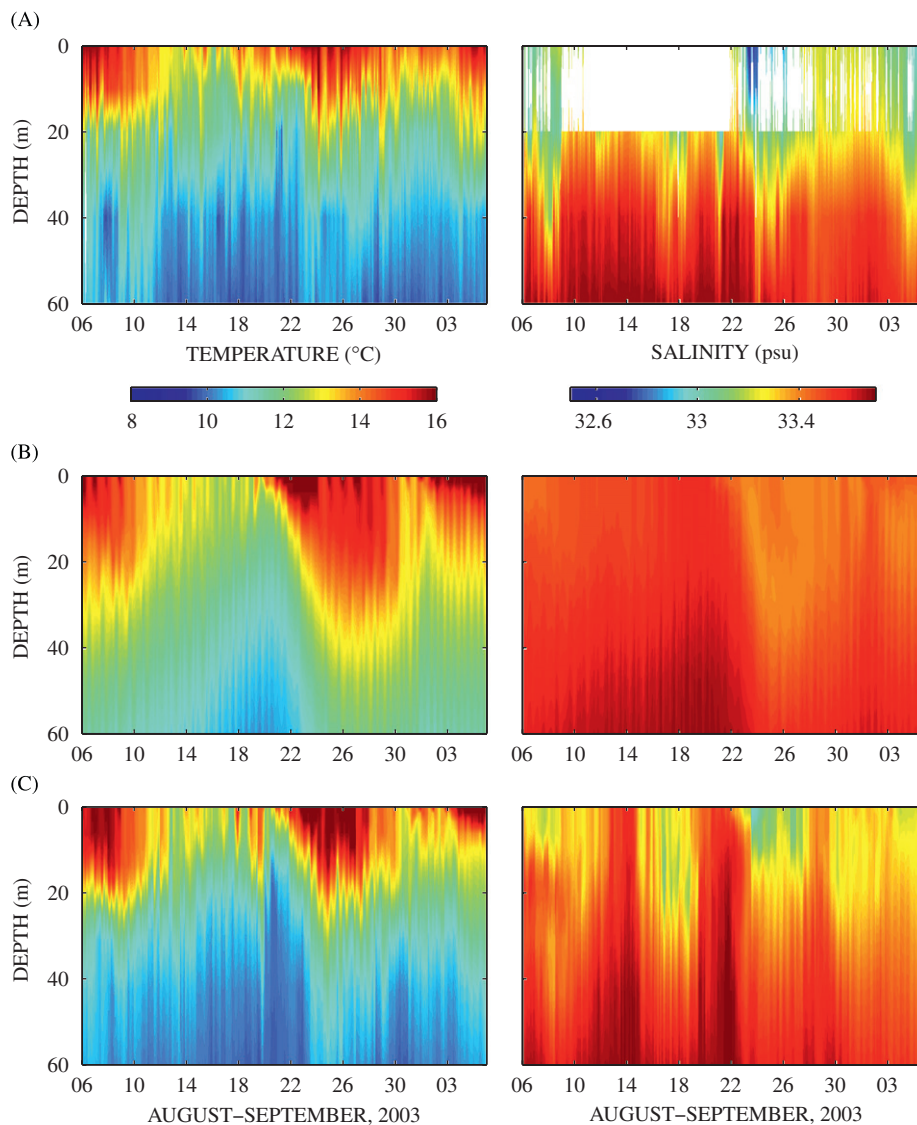


Fig. 11. Comparisons of observed and model-predicted subsurface temperature and salinity at mooring M1: (A) observed; (B) Run 1 (no assimilation); (C) Run 3 (with glider assimilation).

during the brief relaxation events of August 20–22 and September 1–3. The non-assimilative Run 1 shows these transitions (Figs. 11 and 12, middle panel) in subsurface temperature; however, changes are not as defined as in observations. For salinity, the non-assimilating Run 1 significantly differs from the observations. The glider data assimilating Run 3 shows comparable results with observations in deepening (shallowing) of thermocline as well as halocline depths during upwelling (relaxation) events in the Monterey Bay area (bottom panels of Figs. 11 and 12).

Table 4 presents estimates of anomaly correlation (AC) and RMS error between observed and model subsurface temperature and salinity profiles (Figs. 11 and 12) for Runs 1 and 3. AC is estimated from

$$AC = \frac{\sum_G (M - \bar{M})(O - \bar{O})}{\sqrt{\sum_G (M - \bar{M})^2} \sqrt{\sum_G (O - \bar{O})^2}}, \quad (1)$$

where M and O are corresponding model and observed temperature or salinity profiles, \bar{M} and \bar{O} are means over time of observed and model subsurface temperature or salinity profiles, and G denotes the number of grid points. The summation is performed

over depth and time. The RMS is estimated from

$$RMS = \sqrt{\frac{1}{G} \sum_G (M - O)^2}. \quad (2)$$

The assimilation of glider data increased the AC with observations at moorings M1 and M2, especially for subsurface salinity. Also, there is reduction in the RMS error for temperature and salinity for both moorings (for mooring M1 the reduction is almost 50% in RMS error for temperature).

Fig. 13 shows a comparison of the subsurface structure of the U (east–west) and V (north–south) components of observed and model-predicted velocities at mooring M1. U and V components are averaged over the upwelling event of August 15–17 (Fig. 13A) and the relaxation event of August 20–23 (Fig. 13B). Predictions of the alongshore component (V) during the strong upwelling-favorable winds are comparable for runs both with (Run 3) and without assimilation of glider data (Run 1). This can be explained by the good agreement between observed and COAMPS-predicted winds (Fig. 3). The weaker component of the velocity (cross-shore, U component) differs between runs with

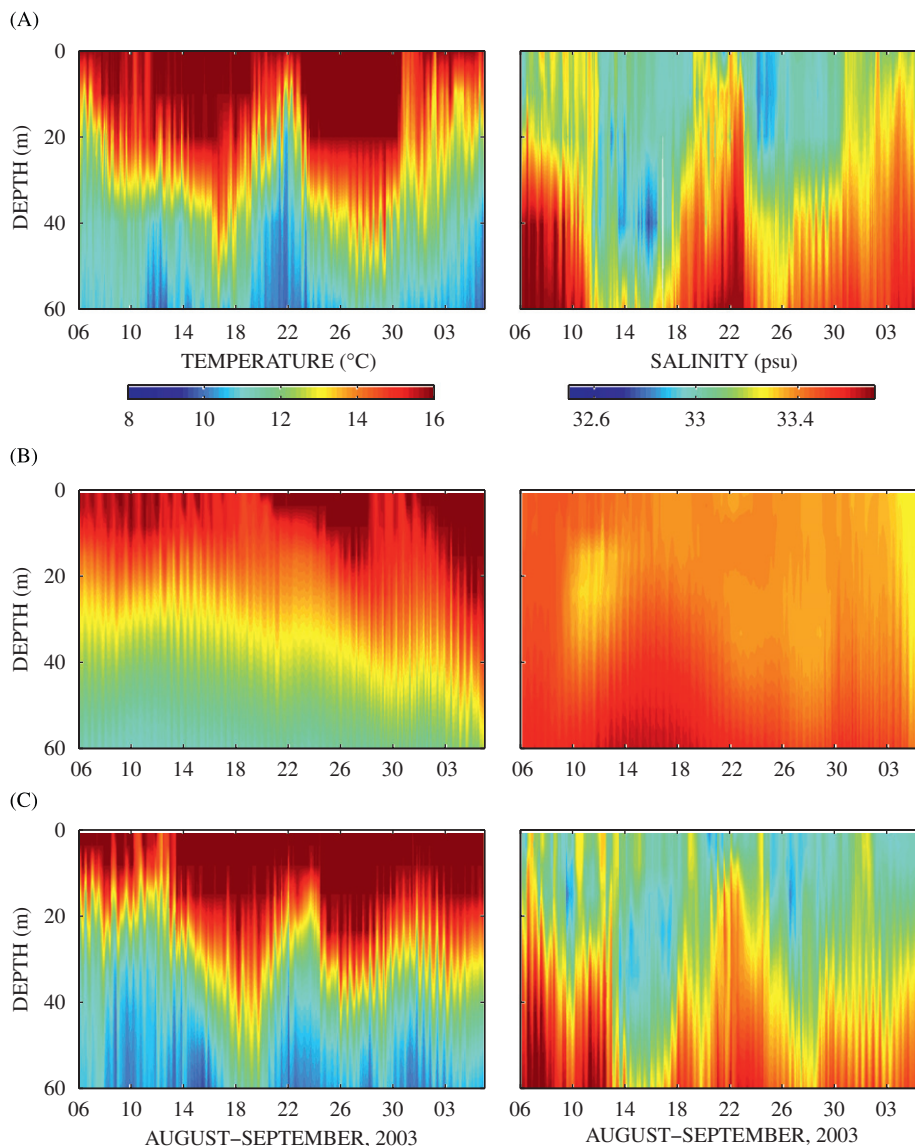


Fig. 12. Same as Fig. 11 but at mooring M2.

Table 4
Anomaly correlation (AC) and RMS for the temperature and salinity depth profiles

Run	Temperature				Run	Salinity			
	M1		M2			M1		M2	
	AC	RMS	AC	RMS		AC	RMS	AC	RMS
1	0.60	1.38	0.03	1.61	1	0.43	0.24	-0.22	0.29
3	0.71	0.76	0.45	1.38	3	0.53	0.17	0.47	0.17

and without assimilation. At the surface, it seems that the run without assimilation is slightly better. However, in deeper water, the run with assimilation is closer to observations. There are considerable deviations between the runs with and without assimilation during the relaxation of wind forcing. There is good agreement between observed and the assimilative Run 3 cross-shore (U) components of velocity for all depths. Also, there is a better agreement with observations in the shape of the vertical

profile of the alongshore component of the velocity for the assimilative Run 3.

To quantify the subsurface comparisons between Runs 1 and 3, complex correlations and angular displacements are estimated for subsurface profiles of velocity (Fig. 13) in accord with Kundu (1976) (Table 5). Complex correlations and angular displacements are comparable for both runs during upwelling because the alongshore components (V) of the velocity for both Runs 1 and 3 are similar during the upwelling event (Fig. 13). During the relaxation event, complex correlation increased from 0.66 (Run 1) to 0.96 (Run 3). At the same time, the averaged angles between observed and model velocity profiles reduced from 92° to -7° .

5. Conclusions and discussions

We evaluated the impact of glider data assimilation on the NCOM model predictions of surface and subsurface properties in the Monterey Bay during the August–September of 2003.

The NCOM model predictions without assimilation of the glider data show that the model predictions of surface properties

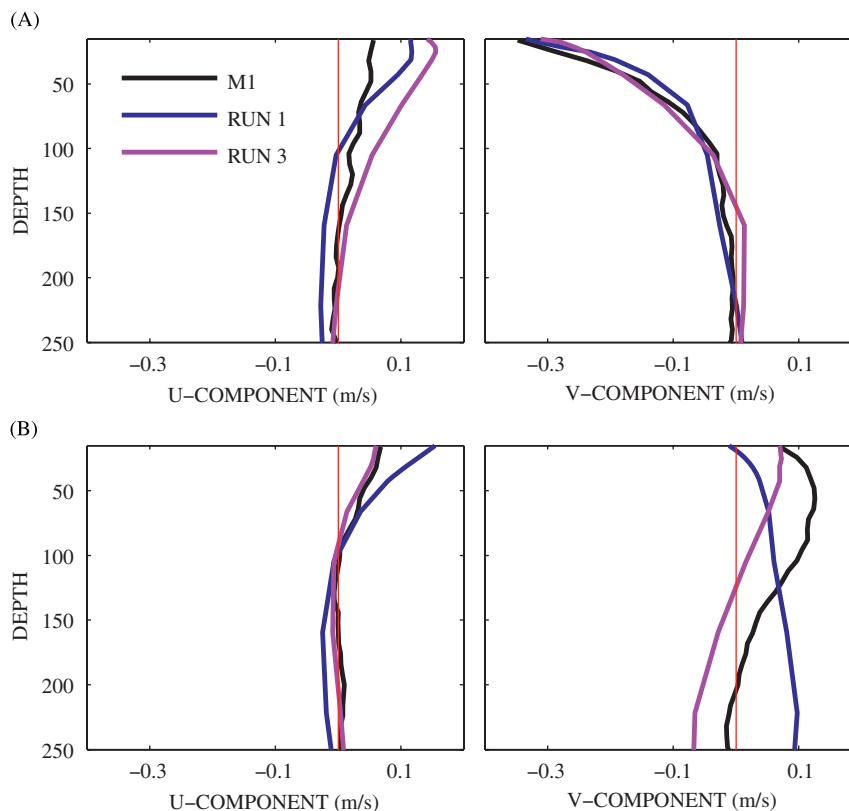


Fig. 13. Comparisons of observed and model-predicted subsurface velocity during (A) upwelling (August 15–17, 2003) and (B) relaxation events (August 20–23, 2003).

Table 5
Complex correlations and angular displacements for subsurface currents profiles

Run	Upwelling		Relaxation	
	Correlation	Angle (°)	Correlation	Angle (°)
1	0.98	–20	0.66	92
3	0.97	–16	0.96	–7

are capable of reproducing the observed sequence of upwelling/relaxation events, and are in reasonably good agreement with observations during strong upwelling-favorable winds. This is a result of the good agreement between the observed and the 3-km resolution atmospheric model COAMPS winds that were used as wind forcing in the non-assimilative run. However, during wind relaxation events, comparisons of observed and model-predicted SSTs at mooring M1 show significant differences: the model-predicted SSTs are much warmer than observed SSTs, and there is stronger diurnal variability in the model-predicted SSTs. These differences between the NCOM model-predicted and observed SSTs are related to the fact that mean daily values of the COAMPS-predicted short-wave radiation (SWR) are about 30–40% larger than the observed values. When SWR values were adjusted to match observed daily values of SWR at mooring M1, the NCOM model predictions were improved and SST bias was reduced.

Even without correction of SWR, the glider data assimilative run (Run 3) was able to reproduce observed SSTs and showed comparable predictions with the Run 2 when SWR was adjusted. Therefore, for hindcasting and nowcasting, the assimilation of the glider data can eliminate deficiencies in model predictions due to the deficiencies in the atmospheric forcing. At the same time, the analysis of the NCOM model predictions revealed that the model

forecast degrades to the level of the model predictions without assimilation in 1–1.5 days. It is shown that for more extended forecasts it is critical to have accurate atmospheric forcing.

Assimilation of glider data provided a better agreement of the model-predicted and observed spatial distributions of SSTs, as for example, in location of warmer and fresher offshore water masses.

Mooring observations present sharp changes in the thermocline and halocline depths during transitions from upwelling to relaxation and visa versa. The glider data assimilating run is able to show improved comparisons with observations in deepening (shallowing) of thermocline as well as halocline depths during upwelling (relaxation) events in the Monterey Bay area.

Comparisons of observed and model-predicted velocities at mooring M1 show that predictions of the alongshore component (V) during the strong upwelling-favorable winds are comparable for both runs with and without assimilation of glider data. This can be explained by the good agreement between observed and COAMPS-predicted winds. During the relaxation of wind, the data assimilative run has higher value of complex correlation with observations than the non-assimilative run.

Our future research will focus on the improvement of the glider data assimilation approach. For example, we will consider the assimilation of threaded glider profiles (when each glider profile has latitude and longitude values changing with the depth) in the framework of the NCODA system. As shown in Figs. 1 and 2, the glider profiles covered the area of M1 and M2 moorings locations well. It is important to evaluate the impact of glider data assimilation in cases when glider observations are away from the area where the model observations comparisons are conducted. During the summer of 2006 experiment in the Monterey Bay, glider profiles were collected to the north of moorings M1 and M2. Evaluations of the model predictions during summer of 2006 and comparisons to predictions during summer of 2003 also will be

the subject of future research. We are also in the process of implementing a new version COAMPS that has demonstrated improved predictive capability for low-level clouds and should provide a more accurate depiction of SWR evolution. Future studies will focus on evaluating SWR predictions from this new version of the model and better understanding the implications for ocean circulation prediction in the Monterey Bay.

Acknowledgments

This research was funded through the Naval Research Laboratory (NRL) under Program Element 61153N sponsored by the Office of Naval Research, and ONR Grants N0001405WX20794 and N0001406WX20990. We thank Peter Sakalaukus of USM for programming and computer support. Computer time for the numerical simulations was provided through a Grant from the Department of Defense High Performance Computing Initiative. Computational resources for COAMPS were supported in part by a Grant of HPC time from the Department of Defense Major Shared Resource Centers, Aberdeen, MD and Wright Patterson Air Force Base, OH. COAMPS is a registered trademark of the Naval Research Laboratory. This manuscript is NRL contribution # 7330-07-7115.

References

- Chavez, F.P., Wright, D., Herlien, R., Kelley, M., Shane, F., Strutton, P.G., 2000. A device for protecting moored spectroradiometers from bio-fouling. *Journal of Atmospheric and Oceanic Technology* 17, 215–219.
- Cummings, J.A., 2006. Operational multivariate ocean data assimilation. *Quarterly Journal of the Royal Meteorological Society* (2005) 131, 3583–3604.
- Doyle, J.D., Jiang, Q., Chao, Y., Farrara, J., 2008. High-resolution real-time modeling of the marine atmospheric boundary layer in support of the AOSNII field campaign. *Deep-Sea Research II*, this issue [doi:10.1016/j.dsr2.2008.08.009].
- Kundu, P.K., 1976. Ekman veering observed near the ocean bottom. *Journal of Physical Oceanography* 6, 238–242.
- Martin, P.J., 2000. Description of the Navy Coastal Ocean Model Version 1.0, NRL/FR/732-00-9962, Naval Research Laboratory, Stennis Space Center, Mississippi.
- Ramp, S.R., Paduan, J.D., Shulman, I., Kindle, J., Bahr, F.L., Chavez, F., 2005. Observations of upwelling and relaxation events in the northern Monterey Bay during August 2000. *Journal of Geophysical Research* 110, C07013.
- Ramp, S.R., Davis, R.E., Leonard, N.E., Shulman, I., Chao, Y., Robinson, A.R., Marsden, J., Lermusiaux, P., Fratantoni, D., Paduan, J.D., Chavez, F., Bahr, F.L., Liang, S., Leslie, W., Li, Z., 2008. Preparing to predict: The second Autonomous Ocean Sampling Network (AOSN-II) experiment in the Monterey Bay. *Deep-Sea Research II*, this issue [doi:10.1016/j.dsr2.2008.08.013].
- Rhodes, R.C., Hurlburt, H.E., Wallcraft, A.J., Barron, C.N., Martin, P.J., Smedstad, O.M., Cross, S., Metzger, J.E., Shriver, J., Kara, A., Ko, D.S., 2002. Navy Real-Time Global Modeling Systems. *Oceanography* 15 (1), 29–43.
- Rosenfeld, L.K., Schwing, F.B., Garfield, N., Tracy, D.E., 1994. Bifurcated flow from an upwelling center: a cold water source for Monterey Bay. *Continental Shelf Research* 14, 931–964.
- Sherman, J., Davis, R.E., Owens, W.B., Valdes, J., 2001. The autonomous underwater glider 'Spray'. *IEEE Oceanic Engineering* 26, 437–446.
- Shulman, I., Wu, C.R., Lewis, J.K., Paduan, J.D., Rosenfeld, L.K., Kindle, J.C., Ramp, S.R., Collins, C.A., 2002. High resolution modeling and data assimilation in the Monterey Bay area. *Continental Shelf Research* 22, 1129–1151.
- Shulman, I., Kindle, J., Derada, S., Anderson, S., Penta, B., Martin, P., 2004. Development of hierarchy of different resolution models for studying US west coast California Current ecosystem. In: Spaulding, M.L. (Ed.), *Estuarine and Coastal Modeling*, Proceedings of 8th International Conference on Estuarine and Coastal Modeling, pp. 74–88.
- Shulman, I., Kindle, J., Martin, P., deRada, S., Doyle, J., Penta, B., Anderson, S., Chavez, F., Paduan, J., Ramp, S., 2007. Modeling of upwelling/relaxation events with the Navy Coastal Ocean Model. *Journal of Geophysical Research* 112, C06023.
- Strutton, P.G., Chavez, F.P., 2004. Biological heating in the equatorial Pacific: observed variability and potential for real-time calculation. *Journal of Climate* 17, 1097–1109.
- Webb, D.C., Simonetti, P.J., Jones, C.P., 2001. Slocum: an underwater glider propelled by environmental energy. *IEEE Journal of Oceanic Engineering* 26, 447–452.